

Chain-of-Thought Textual Reasoning for Few-shot Temporal Action Localization

Hongwei Ji*, Wulian Yun*, Mengshi Qi†, Huadong Ma
 State Key Laboratory of Networking and Switching Technology,
 Beijing University of Posts and Telecommunications, China

Abstract

Traditional temporal action localization (TAL) methods rely on large amounts of detailed annotated data, whereas few-shot TAL reduces this dependence by using only a few training samples to identify unseen action categories. However, existing few-shot TAL methods typically focus solely on video-level information, neglecting textual information, which can provide valuable semantic support for the localization task. Therefore, we propose a new few-shot temporal action localization method by Chain-of-Thought textual reasoning to improve localization performance. Specifically, we design a novel few-shot learning framework that leverages textual semantic information to enhance the model’s ability to capture action commonalities and variations, which includes a semantic-aware text-visual alignment module designed to align the query and support videos at different levels. Meanwhile, to better express the temporal dependencies and causal relationships between actions at the textual level to assist action localization, we design a Chain of Thought (CoT)-like reasoning method that progressively guides the Vision Language Model (VLM) and Large Language Model (LLM) to generate CoT-like text descriptions for videos. The generated texts can capture more variance of action than visual features. We conduct extensive experiments on the publicly available ActivityNet1.3 and THUMOS14 datasets. We introduce the first dataset named Human-related Anomaly Localization and explore the application of the TAL task in human anomaly detection. The experimental results demonstrate that our proposed method significantly outperforms existing methods in single-instance and multi-instance scenarios. We will release our code, data and benchmark.

1. Introduction

With the rapid development of social media platforms such as TikTok and Instagram, the number of short videos has increased tremendously, creating a significant challenge in

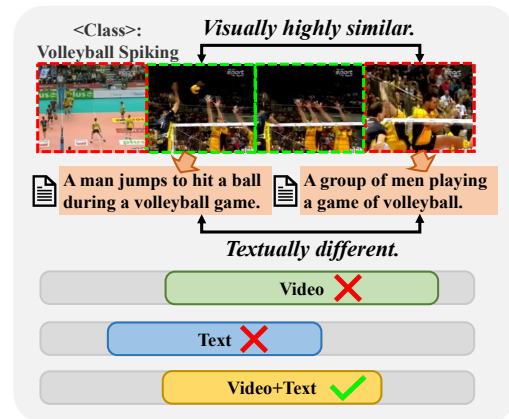


Figure 1. Illustration of the assistance of text information in few-shot TAL task. Existing methods that rely solely on visual information often misjudge when distinguishing between highly similar foreground (green dashed box) and background (red dashed box) snippets. The text provides more semantic details, helping the model achieve more precise prediction.

effectively managing and utilizing large amounts of video resources. Consequently, the importance of video understanding has become more evident. Temporal Action Localization (TAL) [2, 20, 26, 28, 32, 38, 39] as a crucial task in video understanding, aims to detect the start and end times of action instances in untrimmed videos. However, existing TAL methods rely on large amounts of precise temporal annotations for training, requiring substantial data for each category, which is both time-consuming and costly. Furthermore, these methods can only identify action categories present in the training and lack the ability to predict unseen categories, limiting their practical application.

Few-shot learning [3, 4, 9, 18, 27] has shown impressive performance in computer vision tasks, providing a novel solution to the challenges above. By mimicking the human ability to learn from limited labeled samples, models can quickly adapt to new tasks or categories. Few-shot learning can be roughly classified into two categories: meta-learning [4, 9, 18] and transfer learning [3, 6, 27]. Meta-learning enhances the model’s ability to quickly adapt to new tasks by training it on multiple tasks, while transfer learning reduces data requirements by transferring knowl-

* Equal contribution. † Corresponding author: qms@bupt.edu.cn.

edge from existing tasks to new ones. Therefore, few-shot learning is introduced into TAL tasks to enable the model to localize actions in unseen videos using limited data.

Current few-shot TAL methods [13, 14, 17, 23, 34, 35] mainly rely on meta-learning, aligning query and support videos to capture commonalities and variations within the same action category. This enables the model to effectively apply learned knowledge to new classes. However, extracting variations and commonalities from a limited number of video samples becomes challenging. In contrast, textual information explicitly describes the action’s semantic content and context, helping the model more effectively capture its commonalities and variations. Especially, the text description of a short video at various timestamps can bring larger differences than visual appearance. Recent advancements in pre-trained VLM offer a new perspective on this issue. VLM models provide additional prior knowledge by learning joint visual-textual representations from large-scale datasets, particularly in modeling person-object relationships. As shown in Figure 1, the semantic information provided by the text generated by the VLM effectively helps distinguish the athlete’s spike action from ordinary volleyball scenes. Relying solely on visual information, the model finds it challenging to differentiate between these two visually similar contents, which leads to difficulties in accurate localization. Therefore, how to effectively integrate textual information into few-shot TAL tasks, leverage the differences in text representations to overcome the limitations of visual features, enhance the distinction between visually similar content, and improve the consistency between query and support videos remains a challenge.

Furthermore, current methods provide only coarse descriptions of video actions, while the occurrence of actions is often accompanied by temporal dependencies and causal relationships. For example, after a player catches the ball, the next likely action is to shoot. It is still difficult for the model to accurately identify action sequences and their underlying connections. Therefore, generating text that effectively expresses these dependencies and causal relationships to guide few-shot TAL task, thereby enhancing the model’s understanding of dynamic relationships between actions will be promising.

To address the above-mentioned issues, we propose a novel few-shot TAL method, which utilizes textual semantic information to assist the model capture both shared features and variations within the same class, thereby enhancing action localization performance. First, we propose a Chain of Thought (CoT)-like reasoning method, which hierarchically guides VLM and LLM to identify the temporal dependencies of actions and the causal relationships between actions, thereby generating structured CoT-like textual descriptions. Next, we employ a semantic-temporal pyramid encoder and the CLIP text encoder to extract video and

text features across hierarchical levels from the query and support video, and their corresponding text. Subsequently, we design a semantic-aware text-visual alignment module to perform multi-level alignment between videos and texts, leveraging semantic information to capture both commonalities and variations in actions. Finally, the aligned features are fed into the prediction head to generate action proposals. In addition, we explore human-related anomalous events to expand the application scope of few-shot action localization and introduce the first human-related anomaly localization dataset. Our contributions can be summarized as follows:

(1) We introduce a new few-shot learning method, which leverages hierarchical video features with textual semantic information to enhance the alignment of query and support.

(2) We design a CoT-like reasoning method to generate textual descriptions to effectively express temporal dependencies and causal relationships between actions.

(3) We collect and annotate the first benchmark for human-related anomaly localization, which includes 12 types of anomalies and 1,159 videos in total.

(4) We achieve state-of-the-art performance on public benchmarks, attaining improvements of about 4% on the ActivityNet1.3 dataset and 12% on the THUMOS14 dataset under the multi-instance 5-shot scenario compared to the state-of-the-art method.

2. Related Work

Temporal Action Localization aims to locate the start and end times of actions in untrimmed videos. Existing methods can be categorized into two-stage and one-stage methods. Specifically, two-stage methods [2, 21, 26, 28, 37, 39] first estimate potential action proposals, then refine and classify them. Previous studies have primarily focused on generating action proposals, such as classifying anchor windows [2] or detecting action boundaries [21]. Later, some research introduced graph representations [37] or Transformer [28] to further enhance performance. In contrast, one-stage methods [5, 20, 32, 38] simultaneously generate action boundaries and the corresponding labels. However, the above methods rely on a large amount of accurate annotations, making the process both costly and time-consuming, and difficult to generalize to unseen classes.

Few-shot Learning refers to make a model quickly adapt to new categories or tasks with very limited training data, mainly divided into meta-learning [4, 9, 18] and transfer-learning [3, 6, 27]. Considering the similar challenges in TAL, few-shot learning has also been introduced to address these issues. Yang *et al.* [33] first proposes the few-shot TAL, introducing query and support sets to generate action instances by sliding a window over the untrimmed query video. Nag *et al.* [23] employs a query-adaptive Transformer to dynamically adapt to new classes and their corresponding individual videos. Lee *et al.* [17] employs a cross-

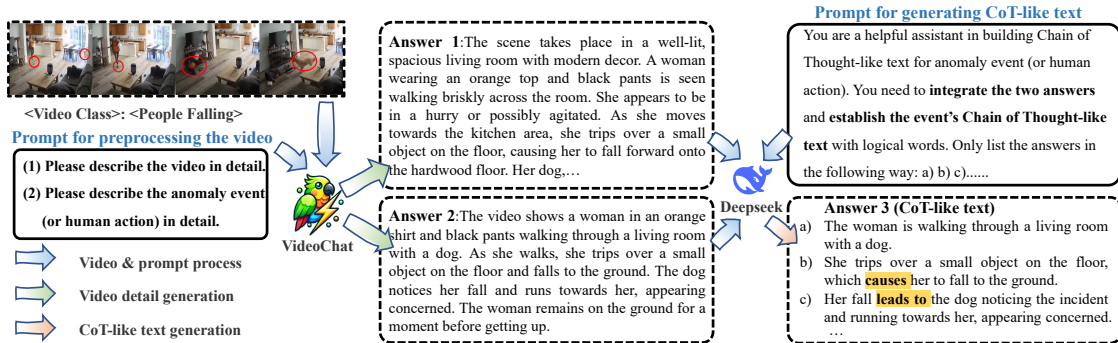


Figure 2. An overview of CoT-like reasoning. We first prompt the VLM to generate details of the video and the process of the human action (or anomaly event) for the given video (\rightarrow). Next, we ask the LLM to generate CoT-like text based on the details and event sequence provided by the VLM (\rightarrow). The logical connectors in the CoT-like text (Answer 3) have been highlighted in yellow.

correlation attention mechanism to dynamically highlight query-relevant frames and suppress irrelevant ones, thereby enhancing the accuracy of action localization. Unlike previous methods that focus solely on aligning the query video and support videos, we integrate textual semantic information to assist in their alignment, thereby enhancing the model’s adaptability to new categories.

3. Human-related Anomaly Localization Benchmark (HAL)

Data source: Current TAL datasets primarily focus on identifying sports and daily activities. However, the task of localizing human anomalous activities is equally significant. Hence, we manually select anomalous videos related to human activities from three large-scale anomaly datasets, namely MSAD [40], XD-Violence [31], and CUVA [7], and construct the Human-related Anomaly Localization dataset. This dataset contains 12 types of human-related anomalous behaviors, such as fighting, people falling, and robbery, as shown in Figure 3. In total, there are 1,161 videos with a cumulative duration of 26.3 hours, comprising over 2,543,000 frames. Each video is accompanied by frame-level annotations of anomaly intervals, along with corresponding frame captions and logical chain text. For more details, please refer to the supplementary materials.

Chain of Thought-like Reasoning: To generate text that adequately represents the temporal dependencies and causal relationships between actions, we propose a CoT-like reasoning method, as shown in Figure 2. Aiming to guide the VLM and LLM through hierarchical steps to gradually generating structured CoT-like textual descriptions, our method processes the task in stages, with each stage refining the previous one, progressively enhancing the understanding of action. First, for each video in the HAL, ActivityNet1.3 [12] and THUMOS14 [15] datasets, we utilize the VLM (i.e., Coca [36]) to generate frame-level captions. This process provides a detailed content foundation for subsequent localization tasks, ensuring that the model can understand

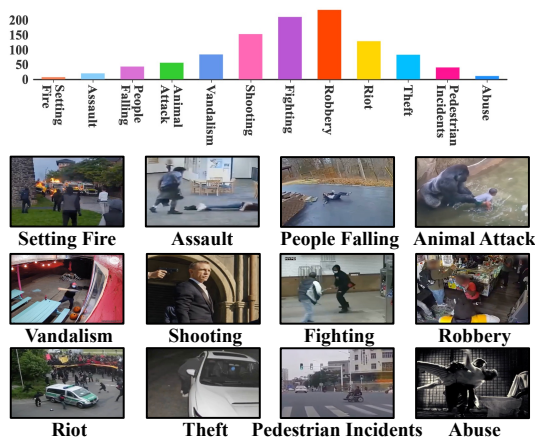


Figure 3. Statistics for the HAL dataset. Mainly contains all the anomaly types along with the corresponding counts.

the semantic information of each frame. Next, we generate the video-level descriptions by guiding the VLM (i.e., VideoChat [19]) with different prompts. This process requires the VLM to capture the details of the video and the overall action sequence, providing an initial context for the video. It helps the model understand the overall structure of the video and identify potential key actions or anomaly events. Building upon this, we further guide the LLM, such as DeepSeek-R1 [10], to perform in-depth logical analysis and reasoning on the generated video-level descriptions, enabling the identification of action sequences and underlying causal relationships. Through this multi-stage generation process, the resulting text progressively presents a structured CoT-like description. Finally, we generate approximately 7,000, 87,000, and 2,400 CoT-like texts for the HAL, ActivityNet1.3, and THUMOS14, respectively.

4. Proposed Method

Problem definition. For the few-shot TAL task, given a training set $D_{\text{train}} = \{(x, y) \mid x \in \mathcal{X}_{\text{train}}, y \in \mathcal{C}_{\text{train}}\}$ and a test set $D_{\text{test}} = \{(x, y) \mid x \in \mathcal{X}_{\text{test}}, y \in \mathcal{C}_{\text{test}}\}$. Specifically, x denotes the input video and $y = (c, t_s, t_e)$ represents labels,

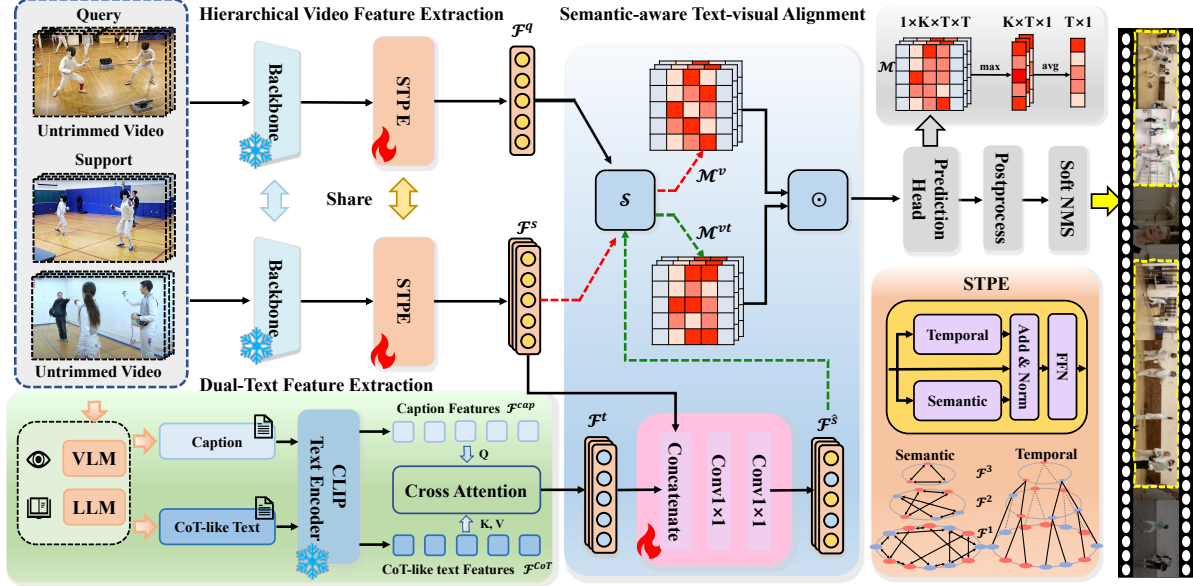


Figure 4. Overall framework of our method. We take three inputs: a query video, a set of support videos, and the corresponding support text generated by the CoT-like reasoning. First, the query video and support videos are processed through a pre-trained backbone, followed by feature extraction using the semantic-temporal pyramid encoder (STPE). Next, the textual features of the support text are extracted using the CLIP Text Encoder. Then, the features from the captions and CoT-like text undergo cross-attention to obtain enhanced textual features. Subsequently, the query video features, support video features, and enhanced textual features are input into the semantic-aware text-visual alignment module. Finally, the aligned features are passed to the prediction head to generate action proposals.

where c denotes the action category, t_s and t_e represent the start and end time of action instance, respectively. Note that the labels of these two sets are disjoint, *i.e.*, $C_{train} \cap C_{test} = \emptyset$. Our goal is to train a model using the training set D_{test} and enable it to localize actions in the test set D_{test} .

Overview. Our proposed few-shot TAL method is shown in Figure 4. First, we perform feature extraction on both the videos and text. Specifically, for input videos, we extract snippet features using a fixed pre-trained backbone *i.e.*, C3D. These extracted features are then passed through our proposed semantic-temporal pyramid encoder to further capture robust temporal and semantic features at multiple hierarchical levels. The corresponding support text is processed using the CLIP Text Encoder to extract semantic information. Then, a semantic-aware text-visual alignment is proposed to improve the model’s ability to capture variations and commonalities within the same class between the query and support videos. Finally, the aligned features are passed to the prediction head to perform localization.

4.1. Hierarchical Video Feature Extraction

Given an untrimmed query video v^q and a set of untrimmed support videos $\{v_i^s\}_{i=1}^K$, where K denotes the number of support videos, we first extract features from all the videos. Specifically, for the query video, we first follow [17, 23] to divide it into multiple non-overlapping snippets $\{v_i^q\}_{i=1}^T$, and then we use the pre-trained C3D [29] as backbone to extract snippet-level features. These features are subse-

quently fed into our proposed Semantic-Temporal Pyramid Encoder to capture more robust features from temporal and semantic levels. Finally, we obtain the feature representation $\mathcal{F}^q \in \mathbb{R}^{1 \times T \times D}$ of the query video, where T denotes the number of snippets and D is the feature dimension. For each support video, we apply the same processing pipeline to obtain the feature representation $\mathcal{F}^s \in \mathbb{R}^{K \times T \times D}$.

Semantic-Temporal Pyramid Encoder. C3D feature primarily focuses on local motion information, neglecting the modeling of long-term temporal dependencies and semantic relationships. As a result, it fails to adequately capture the temporal sequence of actions and their intrinsic connection with the context. To address this, we propose the semantic-temporal pyramid encoder (STPE) to enhance the modeling of both semantic features and long-temporal dependencies at hierarchical levels, as shown in Figure 4.

Our STPE mainly contains a temporal pyramid block and a semantic pyramid block. First, we follow [22] to establish a pyramid structure to obtain feature representations at different scales. Given a video feature $\mathcal{F}^1 = \{f_1^1, f_2^1, \dots, f_T^1\}$ generated by C3D, where f_t^1 , ($t = 1, 2, \dots, T$) denotes the snippet feature, we sequentially perform several snippet-level convolution operations along the temporal dimension of the video features \mathcal{F} , we can extract feature sequences at various scales, which can be expressed as follows:

$$\mathcal{F}^{k+1} = \{\Theta(f_1^k, f_2^k, f_3^k), \Theta(f_4^k, f_5^k, f_6^k), \dots\}, \quad (1)$$

where Θ represents the convolution layer with a kernel size

of 3 and a stride of 3, and $\mathcal{F}^{k+1} \in \mathbb{R}^{(T/3^k) \times D}$ ($k = 1, 2, \dots$) represents the features after k snippets-level convolution operations. Subsequently, we stack these feature sequences to form the pyramid structure, as illustrated in Figure 4. For each feature f_t^1 in \mathcal{F}^1 , we compute the temporal attention by considering its adjacent features $\{f_{t-1}^1, f_{t+1}^1\}$ in the same layer, as well as the feature $f_{\lfloor \frac{t+1}{3} \rfloor}^2 = \Theta(f_{t-1}^1, f_t^1, f_{t+1}^1)$ from the subsequent layer obtained through convolution using the Eq.1. The same attention operation is also performed for other features in the same layer and the higher layers.

However, relying solely on long-term temporal modeling is insufficient for accurately localizing action boundaries, as it fails to capture the intrinsic contextual connections. Therefore, we propose the semantic pyramid block to explore the semantic relationships between snippets. For each feature f_t^k in \mathcal{F}^k , we only need to focus on the m most similar features $\mathcal{F}^{sim} \in \mathbb{R}^{m \times D} = \{f_a^1, f_b^1, \dots\}$ within the same layer to perform a semantic attention operation. This approach not only helps reduce the computational burden but also enhances the discrimination among features. The learning process can be formulated as:

$$Attn(f_t^k) = softmax\left\{\frac{f_t^k W_Q}{\sqrt{D}} (\mathcal{F}^{sim} W_K)^T\right\} (\mathcal{F}^{sim} W_V), \quad (2)$$

where W_Q, W_K, W_V are learnable parameters and D is the feature dimension. The semantic pyramid block enhances the semantic connections across different snippet scales, consolidating commonalities and strengthening variations within the class. After processing through the two pyramids, a residual connection and a feed-forward neural network are applied. Finally, we obtain the query video features \mathcal{F}^q and support video features \mathcal{F}^s .

4.2. Dual-Text Feature Extraction

For the video in the support set, we pre-generate the frame-level captions and CoT-like textual descriptions utilizing the VLM and LLM. Subsequently, the above descriptions are processed through the CLIP Text Encoder [25] to extract the corresponding caption features $\mathcal{F}^{cap} \in \mathbb{R}^{1 \times K \times T \times D}$ and CoT-like text features $\mathcal{F}^{CoT} \in \mathbb{R}^{1 \times K \times T' \times D}$. To combine the temporal nature of the caption features with the coherence and comprehensiveness of the CoT-like text features, we apply cross-attention between the two to generate the final text feature $\mathcal{F}^t \in \mathbb{R}^{1 \times K \times T \times D}$ for assisting the TAL task, which can be formulated as:

$$\mathcal{F}^t = softmax\left\{\frac{\mathcal{F}^{cap} W_Q}{\sqrt{D}} (\mathcal{F}^{CoT} W_K)^T\right\} \cdot (\mathcal{F}^{CoT} W_V), \quad (3)$$

where W_Q, W_K, W_V are learnable parameters and D is the feature dimension. This approach enables us to effectively combine these two types of features while preserving the

temporal sequence of the caption features and introducing greater coherence and comprehensiveness.

4.3. Semantic-aware Text-visual Alignment

After obtaining the video feature representations of the query and support, as well as the text features, denoted \mathcal{F}^q , \mathcal{F}^s , and \mathcal{F}^t . We design a semantic-aware text-visual alignment module consisting of two parts: alignment between video features and the alignment between video features and textual information.

We first align the video features \mathcal{F}^q and \mathcal{F}^s of query and support, where we utilize cosine similarity to measure the degree of alignment between a query-support snippet pair, resulting in the video alignment map $\mathcal{M}^v \in \mathbb{R}^{1 \times K \times T \times T}$. The process can be formulated as the following:

$$\mathcal{M}^v = \mathcal{S}(\mathcal{F}^q, \mathcal{F}^s), \quad (4)$$

where \mathcal{S} denotes cosine similarity. However, solely relying on \mathcal{M}^v to align the query and support action snippets may result in inaccurate alignments, particularly when snippet pairs are irrelevant but share highly similar action backgrounds. Hence, we introduce textual information that can explicitly describe the action and background context, aiding in the capture of commonalities and variations.

We align the support text features \mathcal{F}^t with the support video features \mathcal{F}^s to obtain video-text aligned feature $\mathcal{F}^{\hat{s}} \in \mathbb{R}^{K \times T \times D}$ of support video. We first concatenate the features from two modalities along the feature dimension and then apply two 1×1 convolutions for alignment, which are formulated as:

$$\mathcal{F}^{\hat{s}} = \Theta(\sigma(\Theta(\mathcal{F}^t \oplus \mathcal{F}^s))), \quad (5)$$

where Θ denotes the convolution operation, σ represents the ReLU activation function, and \oplus means the concatenation along the feature dimension. In this way, we align the features from both modalities, enriching the support set and providing additional auxiliary information for the subsequent query and support video alignment. Subsequently, to align between the video features \mathcal{F}^q of query and video-text aligned feature $\mathcal{F}^{\hat{s}}$ of the support, we calculate the video-text alignment map $\mathcal{M}^{vt} \in \mathbb{R}^{1 \times K \times T \times T}$ in the same manner as \mathcal{M}^v :

$$\mathcal{M}^{vt} = \mathcal{S}(\mathcal{F}^q, \mathcal{F}^{\hat{s}}). \quad (6)$$

Relying solely on the video alignment map \mathcal{M}^v to align the query and support can easily lead to the misalignment of visually similar foreground and background snippets. In contrast, the video-text alignment map \mathcal{M}^{vt} leverages the clarity of textual semantics to reduce such occurrences. Therefore, we perform an element-wise multiplication of the two maps, using the video-text alignment map \mathcal{M}^{vt} to correct the erroneous regions in the video alignment map

\mathcal{M}^v . Besides, the background snippets often vary significantly across different support samples, so we concentrate on aligning action commonalities within the foreground snippets by applying background snippets masking operation on the alignment map. Finally, the entire process can be formulated as:

$$\mathcal{M} = \mathcal{M}^v \odot \mathcal{M}^{vt} \odot \mathcal{M}^m, \quad (7)$$

where $\mathcal{M} \in \mathbb{R}^{1 \times K \times T \times T}$, \odot denotes the element-wise multiplication and \mathcal{M}^m is the background snippets mask matrix. Subsequently, we utilize a prediction head to obtain the snippet-level prediction $\hat{p} \in \mathbb{R}^{1 \times T}$.

4.4. Optimization and Inference

Loss function. To optimize our network, we follow [11] to employ the cross-entropy loss, which consists of two snippet-level losses \mathcal{L}_{fg} and \mathcal{L}_{bg} . The total loss function \mathcal{L} is defined as follows:

$$\mathcal{L} = \mathcal{L}_{fg} + \mathcal{L}_{bg}. \quad (8)$$

For better classifying the foreground snippet when there are only a few foreground or background snippets present in a query video during the training, we introduce k_{fg} and k_{bg} to deal with the unbalanced issue as the following:

$$k_{fg} = \min(t, \frac{t}{t_{fg} + \varepsilon}), \quad (9)$$

$$k_{bg} = \min(t, \frac{t}{t_{bg} + \varepsilon}), \quad (10)$$

where t , t_{fg} and t_{bg} are the number of total snippets, foreground snippets, and background snippets, respectively. Additionally, minimum operation and ε are used to avoid situations with excessively large k and where the divisor is zero. With the adjustment ratios k_{fg} and k_{bg} , the two snippet-level loss functions can be described as:

$$\mathcal{L}_{fg} = -k_{fg} \sum_{i=1}^t y(i) \log[\hat{p}(I)], \quad (11)$$

$$\mathcal{L}_{bg} = -k_{bg} \sum_{i=1}^t [1 - y(i)] \log[1 - \hat{p}(I)], \quad (12)$$

where y is the query ground truth mask and $\hat{p} \in \mathbb{R}^{1 \times T}$ represents the snippet-level prediction.

Inference. During the inference phase, we randomly select a novel class from C_{test} , which has never been seen before. For each selected class, we choose $1+k$ video as query and support to form a k -shot localization task, along with the action segment annotations of the support. For every query video, we generate the foreground probability of each snippet by applying the frozen model. Subsequently, we select

the consecutive snippets as proposals where the foreground probability exceeds a predefined threshold. Additionally, we filter out the too-short proposals and calculate the average probability as confidence for the remaining proposals. We then refine the proposals using soft non-maximum suppression (NMS) [1] with a threshold of 0.7.

5. Experiments

5.1. Datasets and Evaluation Metrics

ActivityNet1.3 [12] covers 200 actions, containing 19,994 untrimmed videos with temporal action segment annotations. Following previous work [8], we split the 200 classes into three subsets without any overlap for training (80%), validation (10%) and testing (10%), respectively. For the single-instance scenario, we adopt videos that contain one action segment. For multi-instance scenarios, we utilize the original videos after filtering out those that contain more than one class category. Hence, we remove the videos with invalid links, leaving approximately 16,800 videos.

THUMOS14 [15] covers 20 action categories, with 200 validation videos and 213 test videos. We reconstruct the dataset division for the meta-learning strategy as in [34]. The ratio of the number of training, validation, and test classes follows the same proportions as in ActivityNet1.3. Due to the scarcity of single-instance videos in the original THUMOS14 data, we divide the multi-instance video into several non-overlapping segments, each of which will be regarded as a new single-instance video. Under the multi-instance setting, we continue to use the initial video from THUMOS14, the same as we did for ActivityNet1.3.

Evaluation Metrics. We utilize the mean average precision (mAP) as an evaluation metric to assess the performance of our method, consistent with prior work [17], and report mAP at an IoU threshold of 0.5.

5.2. Implementation Details

We follow [17] to split each video into multiple non-overlapping snippets, and then use the pre-trained C3D [29] network to extract features. We adopt the Adam optimizer [16] with the learning rate of 1e-6 to train the model, implemented in the PyTorch [24] framework on a NVIDIA A6000 GPU. For the ActivityNet1.3 dataset, we train 200 epochs and the batch size is set to 100. Each epoch consists of 100 episodes. For the THUMOS14 dataset, we train 100 epochs and the batch size is set to 20. Each epoch consists of 50 episodes. For the HAL dataset, we train 150 epochs and the batch size is set to 30. Each epoch consists of 50 episodes. During the validation and testing phase, we configure 1000 episodes, 100 episodes, and 500 episodes for ActivityNet1.3, THUMOS14, and HAL. A video consisting of 256 snippets takes 0.2 seconds to inference.

Method	ActivityNet1.3				THUMOS14			
	Single-instance		Multi-instance		Single-instance		Multi-instance	
	1-shot	5-shot	1-shot	5-shot	1-shot	5-shot	1-shot	5-shot
Feng <i>et al.</i> [8]	43.5	-	31.4	-	34.1	-	4.3	-
Yang <i>et al.</i> [34]	53.1	56.5	42.1	43.9	48.7	51.9	7.5	8.6
Yang <i>et al.</i> [35]	57.5	60.6	47.8	48.7	-	-	-	-
Nag <i>et al.</i> [23]	55.1	63.0	44.1	48.2	49.2	54.3	7.3	10.4
Hu <i>et al.</i> [14]	41.0	45.4	29.6	38.9	-	42.2	-	6.8
Hsieh <i>et al.</i> [13]	60.7	61.2	-	-	-	-	-	-
Lee <i>et al.</i> [17]	63.1	67.5	49.4	54.6	55.0	60.5	10.2	16.2
Ours	65.1	71.7	53.9	56.7	54.1	62.6	14.1	18.2

Table 1. Comparison with the state-of-the-art methods in terms of mAP@0.5 on ActivityNet1.3 and THUMOS14 datasets, under both single-instance and multi-instance settings. The best results are highlighted in bold.

Method	1-shot		5-shot	
	0.5	Mean	0.5	Mean
Base	5.9	2.6	14.6	8.1
Transformer	32.4	20.4	34.6	21.2
Ours	38.9	25.2	40.0	26.7

Table 2. Comparison with the baseline and Transformer in terms of mAP@0.5 and mean mAP on HAL dataset.

Method	STPE	Text	Multi-instance	
			1-shot	5-shot
Base			7.6	10.6
Base + STPE	✓		8.6	13.0
Base + Text		✓	13.0	14.6
Ours	✓	✓	14.1	18.2

Table 3. Ablation study of our method on THUMOS14. ‘Base’ indicates baseline, ‘STPE’ denotes the semantic-temporal pyramid encoder, and ‘Text’ represents textual information.

Method		1-shot		5-shot	
		0.5	Mean	0.5	Mean
STPE	w/o STPE	13.0	4.2	14.6	4.9
	w/o TP	13.5	4.2	17.1	5.0
	w/o SP	13.7	4.8	17.6	5.5
	Transformer	13.4	4.6	16.7	5.3
Text	Prompt	12.5	3.4	14.5	5.3
	Caption	12.9	4.6	16.4	5.4
Alignment	VV	11.3	3.5	13.8	4.2
	VT	12.4	4.9	13.4	5.3
	VV+VT	8.5	2.7	15.8	4.8
ours		14.1	5.4	18.2	7.3

Table 4. Ablation study on the variants of STPE, text descriptions, and alignment strategies on THUMOS14 dataset.

5.3. Comparison with State-of-the-Art Methods

We compare our method with the state-of-the-art few-shot TAL methods [8, 13, 14, 17, 23, 34, 35] on ActivityNet1.3 and THUMOS14, reporting the performance measured by

mAP at an IoU threshold of 0.5 in Table 1. Additionally, we compare our method with a Transformer of comparable parameter size on the HAL dataset and report the mAP@0.5 and mean mAP in Table 2.

ActivityNet1.3. Our method consistently outperforms existing few-shot TAL methods in single-instance and multi-instance scenarios across 1-shot and 5-shot settings. In the multi-instance 5-shot case, it achieves 56.7 mAP@0.5, while in the single-instance 1-shot setting, it reaches 71.7 mAP@0.5. This performance can be attributed to two key factors: First, we extract hierarchical features from temporal and semantic dimensions, allowing better localization of action regions and enhancing semantic relationships. Additionally, incorporating textual information improves the model’s ability to capture class variations and commonalities, further enhancing alignment and localization.

THUMOS14. As shown in Table 1, our method achieves competitive results across various settings, particularly in the multi-instance 1-shot and 5-shot scenarios, where it improves upon Lee *et al.*[17] by 24.6% and 38.2%, respectively. In the single-instance 1-shot scenario, mAP@0.5 declines slightly because the single-instance segments in THUMOS14 are individually extracted from multi-instance videos. Each segment has an incomplete action and a short duration, which hinders our CoT-like text from providing comprehensive guidance on action sequences.

HAL. Table 2 presents our results on the HAL dataset. As shown in the table, our method outperforms the Transformer by 6% in mAP@0.5 and by 5% in mean mAP. This is mainly because the CoT-like text provides a completely logical process of the occurrence of abnormal events, thereby helping the model better locate the anomalous segments.

5.4. Ablation Study

Impact of different components. We evaluate the impact of different components of our method under a multi-instance scenario on the THUMOS14 and report the mAP@0.5 in Table 3. First, we establish our baseline model by removing the STPE and all operations involving textual

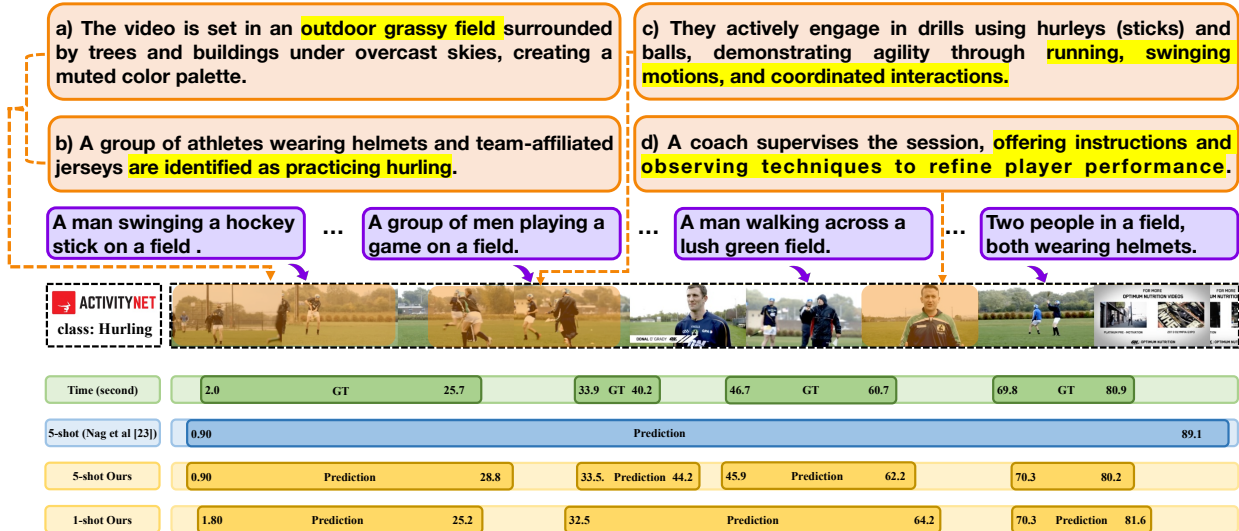


Figure 5. Qualitative comparisons of our method, QAT [23] and Ground Truth on “Hurling” from Activity1.3. The text in purple denote the captions, and the orange text present the CoT-like content. While captions provide brief scene descriptions, the CoT-like text offer a more consistent and comprehensive textual narrative. By combining these two forms of text, the model can better localize the action segments.

information. Subsequently, we gradually add the STPE and textual information to the baseline. As shown in the table, the results improve with the addition of different modules, demonstrating the effectiveness of the various components proposed in this paper.

Impact of semantic-temporal pyramid encoder. We evaluate the impact of different variants of STPE, with mAP@0.5 presented in the ‘STPE’ section of Table 4. The following variants are considered: 1) w/o STPE: remove the STPE and use only the backbone for feature extraction; 2) w/o TP: utilize only the semantic pyramid block of STPE; 3) w/o SP: utilize only the temporal pyramid block of STPE; 4) Transformer: replace the STPE with the Transformer [30], which has comparable parameters for feature extraction. The results in Table 4 indicate that removing either the semantic or temporal pyramid block leads to a decline in performance. Notably, completely removing STPE causes a significant drop. In comparison, our approach outperforms the Transformer, demonstrating that robust feature extraction from both semantic and temporal dimensions significantly enhances action localization performance.

Impact of different textual content. We compare our text generation approach with other methods that generate prompts based on category information and those using only frame-level captions. As shown in Table 4, our method outperforms both approaches across various settings and metrics. This improvement can be attributed to the comprehensive CoT-like text, which provides auxiliary information on causal and contextual relationships between actions. This richer context enhances the model’s alignment capabilities, leading to improved performance.

Impact of semantic-aware text-visual alignment. We

evaluate the impact of different alignment strategies within the semantic-aware text-visual alignment, with mAP@0.5 reported in Table 4. We assess three alignment strategies: 1) Video align Video (VV): align only the query video features with the support video features during operation \mathcal{S} ; 2) Video align Text (VT): align the query video features with support features that have been aligned with text during operation \mathcal{S} ; 3) Video + Text (VV+VT): aligns the query video features with support features that have been aligned with text during operation \mathcal{S} . The results indicate that incorporating textual semantic information for alignment outperforms methods relying solely on video information. Among the strategies evaluated, our approach leveraging both video and text information yields the best results. Furthermore, using multiplication in our method is more effective than direct addition, as it refines the incorrect alignment in \mathcal{M}^v by multiplying it with the correct alignment score in \mathcal{M}^{vt} derived from the auxiliary textual information.

5.5. Qualitative Analysis

To prove the effectiveness of our method, we show qualitative results of two cases from the ActivityNet1.3 dataset in Figure 5. We observe that our method (yellow background boxes) locates the action segments more accurately than QAT [23] (blue background box) under a 5-shot setting. Furthermore, our method maintains performance comparable to that of the 5-shot setting, even in the 1-shot scenario.

6. Conclusion

In this paper, we present a novel few-shot TAL method that integrates textual semantic information to enhance action localization performance. First, we designed a CoT-like

reasoning method to generate textual descriptions that can express temporal dependencies and causal relationships between actions. Then, a novel few-shot learning framework was designed to capture hierarchical action commonalities and variations by aligning query and support videos. And the first Human-related Anomaly Localization Benchmark was collected. Extensive experiments demonstrate the effectiveness and superiority of our proposed method.

References

- [1] Navaneeth Bodla, Bharat Singh, Rama Chellappa, and Larry S Davis. Soft-nms—improving object detection with one line of code. In *Proceedings of the IEEE international conference on computer vision*, pages 5561–5569, 2017. 6
- [2] Shyamal Buch, Victor Escorcia, Chuanqi Shen, Bernard Ghanem, and Juan Carlos Niebles. Sst: Single-stream temporal action proposals. In *2017 IEEE Conference on Computer Vision and Pattern Recognition (CVPR)*, pages 6373–6382, 2017. 1, 2
- [3] Wei-Yu Chen, Yen-Cheng Liu, Zsolt Kira, Yu-Chiang Frank Wang, and Jia-Bin Huang. A closer look at few-shot classification. *arXiv preprint arXiv:1904.04232*, 2019. 1, 2
- [4] Yinbo Chen, Zhuang Liu, Huijuan Xu, Trevor Darrell, and Xiaolong Wang. Meta-baseline: Exploring simple meta-learning for few-shot learning. In *Proceedings of the IEEE/CVF international conference on computer vision*, pages 9062–9071, 2021. 1, 2
- [5] Feng Cheng and Gedas Bertasius. Tallformer: Temporal action localization with a long-memory transformer. In *Computer Vision – ECCV 2022*, pages 503–521, Cham, 2022. Springer Nature Switzerland. 2
- [6] Guneet S Dhillon, Pratik Chaudhari, Avinash Ravichandran, and Stefano Soatto. A baseline for few-shot image classification. *arXiv preprint arXiv:1909.02729*, 2019. 1, 2
- [7] Hang Du, Sicheng Zhang, Binzhu Xie, Guoshun Nan, Jiayang Zhang, Junrui Xu, Hangyu Liu, Sicong Leng, Jiangming Liu, Hehe Fan, Dajiu Huang, Jing Feng, Linli Chen, Can Zhang, Xuhuan Li, Hao Zhang, Jianhang Chen, Qimei Cui, and Xiaofeng Tao. Uncovering what, why and how: A comprehensive benchmark for causation understanding of video anomaly. In *2024 IEEE/CVF Conference on Computer Vision and Pattern Recognition (CVPR)*, pages 18793–18803, 2024. 3
- [8] Yang Feng, Lin Ma, Wei Liu, Tong Zhang, and Jiebo Luo. Video re-localization. In *Proceedings of the European Conference on Computer Vision (ECCV)*, pages 51–66, 2018. 6, 7
- [9] Chelsea Finn, Pieter Abbeel, and Sergey Levine. Model-agnostic meta-learning for fast adaptation of deep networks. In *International conference on machine learning*, pages 1126–1135. PMLR, 2017. 1, 2
- [10] Daya Guo, Dejian Yang, Haowei Zhang, Junxiao Song, Ruoyu Zhang, Runxin Xu, Qihao Zhu, Shirong Ma, Peiyi Wang, Xiao Bi, et al. Deepseek-r1: Incentivizing reasoning capability in llms via reinforcement learning. *arXiv preprint arXiv:2501.12948*, 2025. 3
- [11] Bo He, Xitong Yang, Le Kang, Zhiyu Cheng, Xin Zhou, and Abhinav Shrivastava. Asm-loc: Action-aware segment modeling for weakly-supervised temporal action localization. In *Proceedings of the IEEE/CVF conference on computer vision and pattern recognition*, pages 13925–13935, 2022. 6
- [12] Fabian Caba Heilbron, Victor Escorcia, Bernard Ghanem, and Juan Carlos Niebles. Activitynet: A large-scale video benchmark for human activity understanding. In *Proceedings of the IEEE/CVF Conference on Computer Vision and Pattern Recognition*, pages 961–970, 2015. 3, 6
- [13] He-Yen Hsieh, Ding-Jie Chen, Cheng-Wei Chang, and Tyng-Luh Liu. Aggregating bilateral attention for few-shot instance localization. In *Proceedings of the IEEE/CVF Winter Conference on Applications of Computer Vision*, pages 6325–6334, 2023. 2, 7
- [14] Tao Hu, Pascal Mettes, Jia-Hong Huang, and Cees GM Snoek. Silco: Show a few images, localize the common object. In *Proceedings of the IEEE/CVF International Conference on Computer Vision*, pages 5067–5076, 2019. 2, 7
- [15] Yu-Gang Jiang, Jingen Liu, Amir R. Zamir, George Toderici, Ivan Laptev, Mubarak Shah, and Rahul Sukthankar. Thumos challenge: Action recognition with a large number of classes, 2014. <https://www.crcv.ucf.edu/THUMOS14/>. 3, 6
- [16] Diederik P Kingma and Jimmy Ba. Adam: A method for stochastic optimization. *arXiv preprint arXiv:1412.6980*, 2014. 6
- [17] Juntae Lee, Mihir Jain, and Sungrack Yun. Few-shot common action localization via cross-attentional fusion of context and temporal dynamics. In *Proceedings of the IEEE/CVF International Conference on Computer Vision*, pages 10214–10223, 2023. 2, 4, 6, 7
- [18] Kwonjoon Lee, Subhransu Maji, Avinash Ravichandran, and Stefano Soatto. Meta-learning with differentiable convex optimization. In *2019 IEEE/CVF Conference on Computer Vision and Pattern Recognition (CVPR)*, pages 10649–10657, 2019. 1, 2
- [19] Xinhao Li, Yi Wang, Jiashuo Yu, Xiangyu Zeng, Yuhan Zhu, Haiyan Huang, Jianfei Gao, Kunchang Li, Yanan He, Chenting Wang, et al. Videochat-flash: Hierarchical compression for long-context video modeling. *arXiv preprint arXiv:2501.00574*, 2024. 3
- [20] Tianwei Lin, Xu Zhao, and Zheng Shou. Single shot temporal action detection. In *Proceedings of the 25th ACM International Conference on Multimedia*, page 988–996, New York, NY, USA, 2017. Association for Computing Machinery. 1, 2
- [21] Tianwei Lin, Xu Zhao, Haisheng Su, Chongjing Wang, and Ming Yang. Bsn: Boundary sensitive network for temporal action proposal generation. In *Proceedings of the European Conference on Computer Vision (ECCV)*, 2018. 2
- [22] Shizhan Liu, Hang Yu, Cong Liao, Jianguo Li, Weiyao Lin, Alex X Liu, and Schahram Dustdar. Pyraformer: Low-complexity pyramidal attention for long-range time series modeling and forecasting. In *# PLACEHOLDER_PARENT_METADATA_VALUE#*, 2022. 4
- [23] Sauradip Nag, Xiayan Zhu, and Tao Xiang. Few-shot temporal action localization with query adaptive transformer. *arXiv preprint arXiv:2110.10552*, 2021. 2, 4, 7, 8

- [24] Adam Paszke, Sam Gross, Francisco Massa, Adam Lerer, James Bradbury, Gregory Chanan, Trevor Killeen, Zeming Lin, Natalia Gimelshein, Luca Antiga, et al. Pytorch: An imperative style, high-performance deep learning library. *Advances in Neural Information Processing Systems*, 32:8026–8037, 2019. 6
- [25] Alec Radford, Jong Wook Kim, Chris Hallacy, Aditya Ramesh, Gabriel Goh, Sandhini Agarwal, Girish Sastry, Amanda Askell, Pamela Mishkin, Jack Clark, et al. Learning transferable visual models from natural language supervision. In *International conference on machine learning*, pages 8748–8763. PMLR, 2021. 5
- [26] Zheng Shou, Dongang Wang, and Shih-Fu Chang. Temporal action localization in untrimmed videos via multi-stage cnns. In *2016 IEEE Conference on Computer Vision and Pattern Recognition (CVPR)*, pages 1049–1058, 2016. 1, 2
- [27] Qianru Sun, Yaoyao Liu, Tat-Seng Chua, and Bernt Schiele. Meta-transfer learning for few-shot learning. In *2019 IEEE/CVF Conference on Computer Vision and Pattern Recognition (CVPR)*, pages 403–412, 2019. 1, 2
- [28] Jing Tan, Jiaqi Tang, Limin Wang, and Gangshan Wu. Relaxed transformer decoders for direct action proposal generation. In *Proceedings of the IEEE/CVF International Conference on Computer Vision (ICCV)*, pages 13526–13535, 2021. 1, 2
- [29] Du Tran, Lubomir Bourdev, Rob Fergus, Lorenzo Torresani, and Manohar Paluri. Learning spatiotemporal features with 3d convolutional networks. In *2015 IEEE International Conference on Computer Vision (ICCV)*, pages 4489–4497, 2015. 4, 6
- [30] Ashish Vaswani, Noam Shazeer, Niki Parmar, Jakob Uszkoreit, Llion Jones, Aidan N Gomez, Łukasz Kaiser, and Illia Polosukhin. Attention is all you need. In *Advances in neural information processing systems*, pages 5998–6008, Long Beach, CA, USA, 2017. MIT. 8
- [31] Peng Wu, jing Liu, Yujia Shi, Yujia Sun, Fangtao Shao, Zhaoyang Wu, and Zhiwei Yang. Not only look, but also listen: Learning multimodal violence detection under weak supervision. In *European Conference on Computer Vision (ECCV)*, 2020. 3
- [32] Mengmeng Xu, Chen Zhao, David S. Rojas, Ali Thabet, and Bernard Ghanem. G-tad: Sub-graph localization for temporal action detection. In *2020 IEEE/CVF Conference on Computer Vision and Pattern Recognition (CVPR)*, pages 10153–10162, 2020. 1, 2
- [33] Hongtao Yang, Xuming He, and Fatih Porikli. One-shot action localization by learning sequence matching network. In *Proceedings of the IEEE Conference on Computer Vision and Pattern Recognition*, pages 1450–1459, 2018. 2
- [34] Pengwan Yang, Vincent Tao Hu, Pascal Mettes, and Cees GM Snoek. Localizing the common action among a few videos. In *Computer Vision–ECCV 2020: 16th European Conference, Glasgow, UK, August 23–28, 2020, Proceedings, Part VII 16*, pages 505–521. Springer, 2020. 2, 6, 7
- [35] Pengwan Yang, Pascal Mettes, and Cees GM Snoek. Few-shot transformation of common actions into time and space. In *Proceedings of the IEEE/CVF conference on computer vision and pattern recognition*, pages 16031–16040, 2021. 2, 7
- [36] Jiahui Yu, Zirui Wang, Vijay Vasudevan, Legg Yeung, Mojtaba Seyedhosseini, and Yonghui Wu. Coca: Contrastive captioners are image-text foundation models. *arXiv preprint arXiv:2205.01917*, 2. 3
- [37] Runhao Zeng, Wenbing Huang, Mingkui Tan, Yu Rong, Peilin Zhao, Junzhou Huang, and Chuang Gan. Graph convolutional networks for temporal action localization. In *ICCV*, 2019. 2
- [38] Chen-Lin Zhang, Jianxin Wu, and Yin Li. Actionformer: Localizing moments of actions with transformers. In *European Conference on Computer Vision*, pages 492–510, 2022. 1, 2
- [39] Yue Zhao, Yuanjun Xiong, Limin Wang, Zhirong Wu, Xiaoou Tang, and Dahua Lin. Temporal action detection with structured segment networks. In *ICCV*, 2017. 1, 2
- [40] Liyun Zhu, Lei Wang, Arjun Raj, Tom Gedeon, and Chen Chen. Advancing video anomaly detection: A concise review and a new dataset. In *The Thirty-eighth Conference on Neural Information Processing Systems Datasets and Benchmarks Track*, 2024. 3